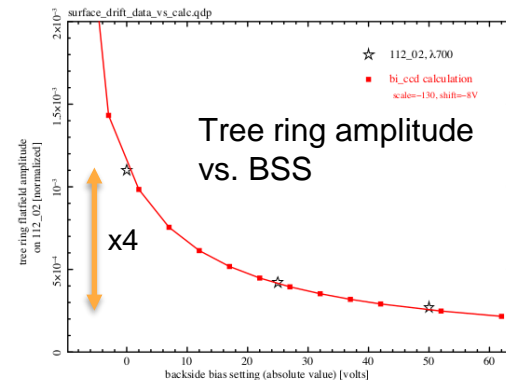
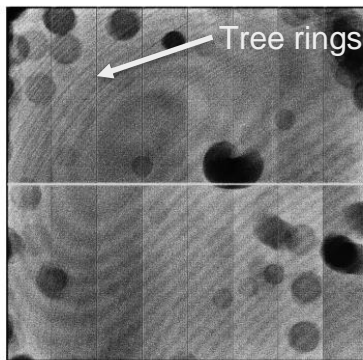
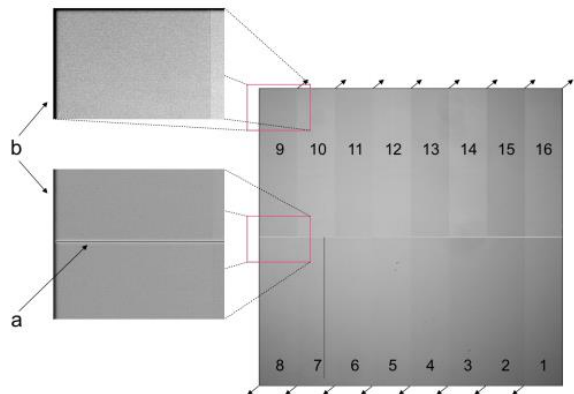


On the influence of electrostatic barriers that would modify brighter-fatter corrections for PSF estimations

Andy Rasmussen & Alex Broughton – ISPA24C41

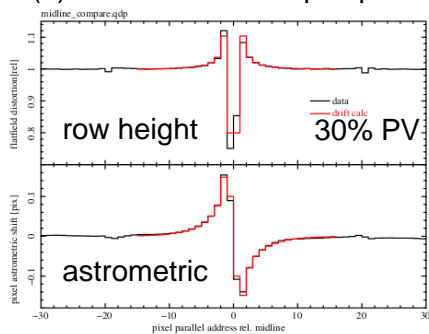
- We use a generic Si drift simulator (https://github.com/arasmssn/bi_ccd_pixpart), operated under cold carrier approximation & validated against all available model-constraining observables to compute pixel boundary response to fixed-pattern & dynamic charge configurations within the pixel. **Linked list** implementation for E-field source management is appropriate for this problem: 10-20 pixel electrostatic field range & trajectory starting point bisection algorithm tolerance ($<10^{-5}$ pixel). (cf. A.Rasmussen 2014 *JINST* **9** C04027).
- This utilizes a non-unique solution to Poisson's equation within the photosensitive volume (depleted of carriers) and uses superposition of electric field sources that are solutions to Gauss's law, method of images are used to approximate planes of symmetry (and equipotential surfaces) e.g. the conductive backside window and polysilicon gate structure in these CCDs.
- Derived solutions for the time being are specific to one flavor of **LSS** focal plane sensor model (Teledyne/e2v-CCD250) operated under design conditions (-70V BSS) & integrating clock swing configuration (cf. Guyonnet et al. 2015).
- Many, many other datasets exist for the 205 devices/3216 amp channels distributed across sensor models & optimized operating conditions (cf. Y. Utsumi, contrib.42). There's a lot to learn from a single operating case, single signal level.



Fixed pattern features: area & astrometric shifts

(a): midline bloomstop implant

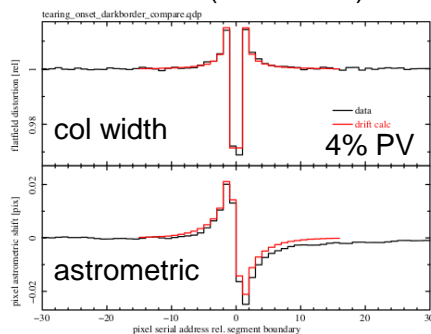
(b): edge rolloff



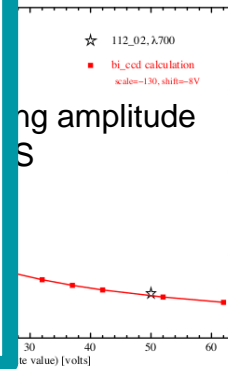
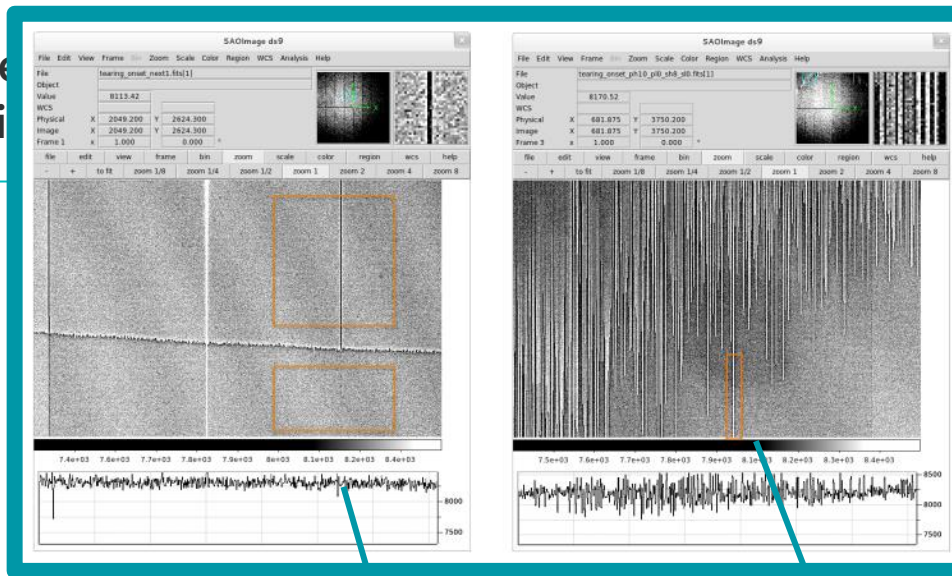
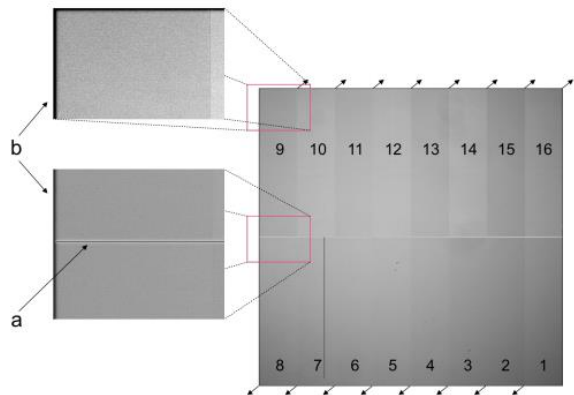
dynamic (tearing) features: area & astrometric shifts

Dark border (Divisadero)

Bright finger (isol. cstop w/holes)



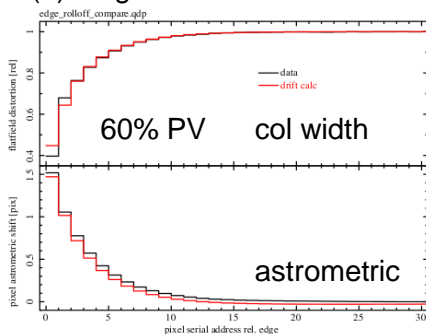
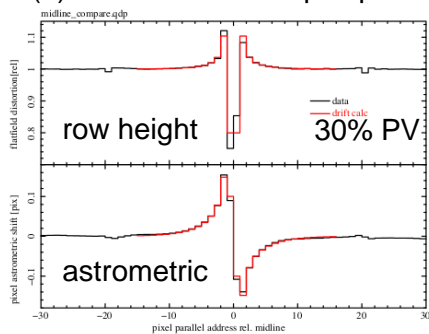
Reconciling observed features & contributions (fixed vs dynamic)



Fixed pattern features: area & astrometric shifts

(a): midline bloomstop implant

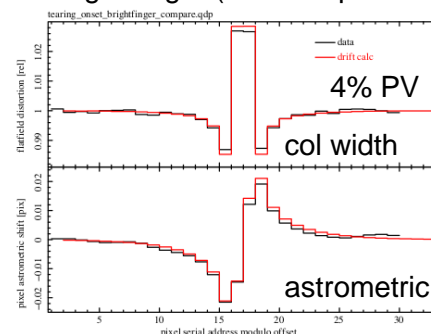
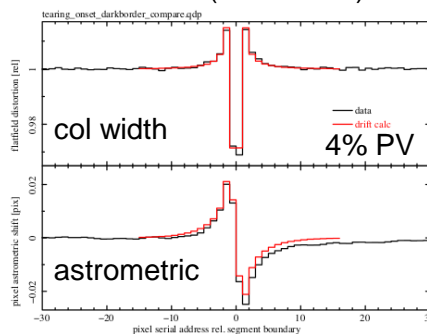
(b): edge rolloff



dynamic (tearing) features: area & astrometric shifts

Dark border (Divisadero)

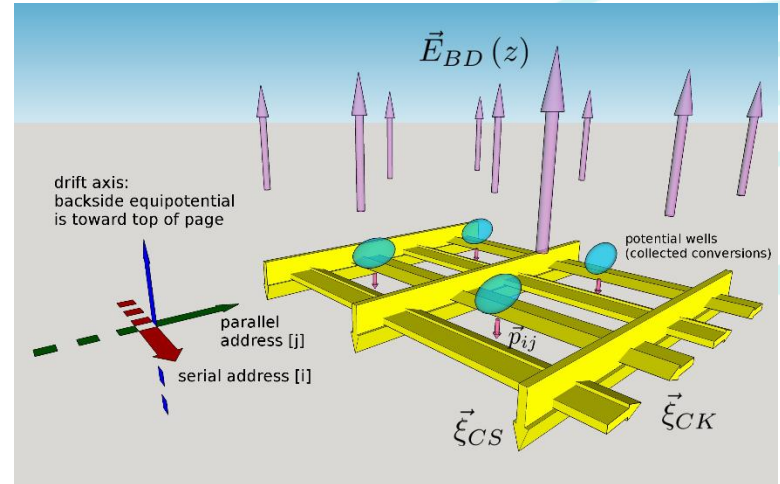
Bright finger (isol. cstop w/holes)

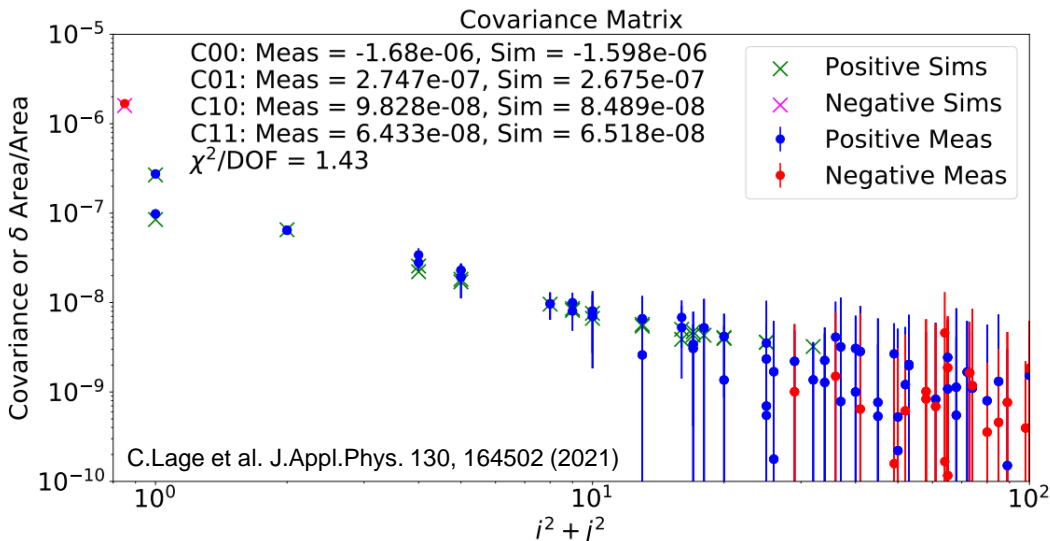


The implementation of this model is represented as a sketchup cartoon (image charge configurations not shown). cf. A.Rasmussen 2015 *JINST* **10** C05028.

- 2x2 pixel region near the channel shown.
- Serial addresses vary along the red coordinate.
- Polysilicon gates form equipotentials extending along this axis.
- Parallel addresses vary along the green coordinate.
- Channel stop barriers form (periodic/infinite) p+ negative charge distributions extending along this axis.
- Non-unique solution to Poisson equation represented by E_{BD} .
- Carriers drift toward the channel (green ovals) from the backside window and partition into pixels. For marginal cases near boundaries, saddle condition is approached. Saddle condition is defined as:

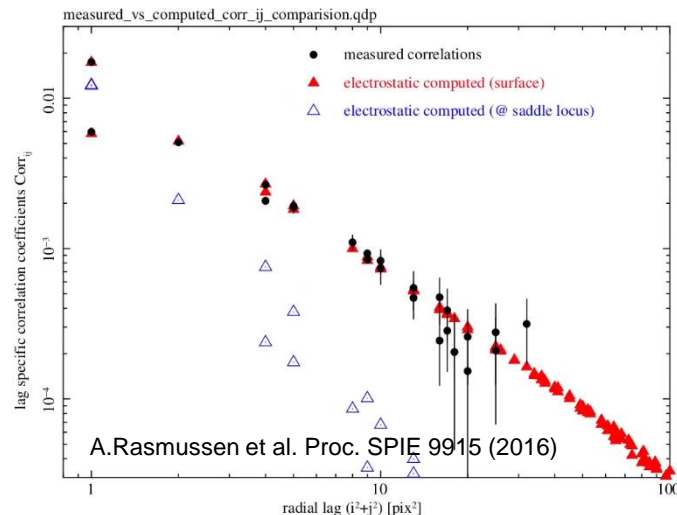
$$\vec{\nabla} \phi = 0 \text{ and } \partial^2 \phi / \partial z^2 < 0 \text{ and } (\partial^2 \phi / \partial x^2 > 0 \text{ or } \partial^2 \phi / \partial y^2 > 0)$$





C_{01} : within 2.7%
 C_{10} : within 15.8%
 C_{11} : within 1.3%

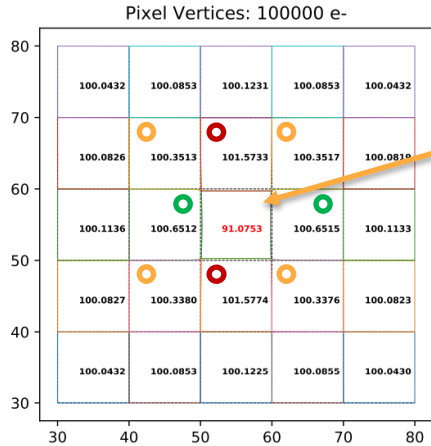
Model (Sims) are based on a combination of destructive diagnostic testing and other parameters finalized on in PoissonCCD config file contents



Corr_{01} : within 0.4%
 Corr_{10} : within 2.4%
 Corr_{11} : within 1.6%

Model (red triangles) are simplex-fit to the data (black dots) to minimize Merit Function. (Free parameters = 3).

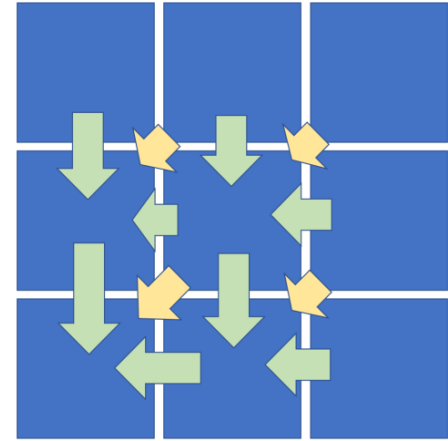
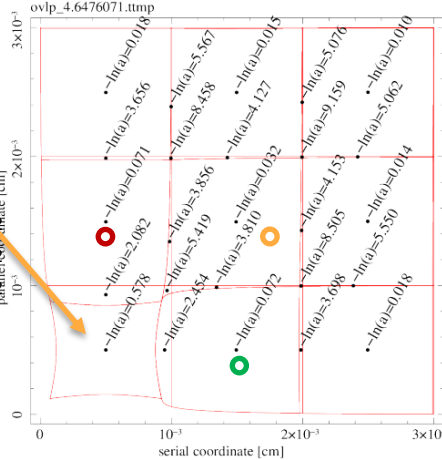
How are the simulations evaluated and compared to observables?



Central pixel containing BFE source signal

BFE lag dependence

- ij=01: $\Delta a_{01}/e^- \sim +2.7e-7$ pix
- ij=10: $\Delta a_{10}/e^- \sim +9.5e-8$ pix
- ij=11: $\Delta a_{11}/e^- \sim +6.5e-8$ pix



C.Lage et al. J.Appl.Phys. 130, 164502 (2021)

A.Rasmussen ISPA (2018)

NB#0: These area distortions are between x400 larger than what is seen in flat fields! $\langle \text{sqrt}(\text{var}) \rangle \sim 240e^-$.

NB#1: area distortions (Δa_{01} etc.) are observable in flat field correlations, while the corrections (M_{0100} etc.) are **not observable**. Recovering them was a primary focus of P.Antilogus et al. 2014 *JINST* **9** C03048, §5.

Pixel boundary formalism (right hand figures) permits analysis of overlaps as corrections e.g. sparse matrix with 4 indices indicating source & destination pairs:

From: (i,j) To: (i',j') and expressed as $M_{ijij'}$.

In this extremely distorted case**,

$$\begin{aligned}
 M_{0100} &\sim 2.22 \times \Delta a_{01} \\
 M_{1000} &\sim 5.22 \times \Delta a_{10} \\
 M_{1110} &\sim 1.36 \times \Delta a_{11} \\
 M_{1101} &\sim 1.30 \times \Delta a_{11}
 \end{aligned}$$

$M_{1100} \sim 0.27 \times \Delta a_{11}$ (scales quadratically, but outside scope of Coulton [2018] algorithm.)

Current, best performance in LSST BFE correction as a part of ISR still shows undesirable artifacts (Broughton et al. 2023)

Sample ITL

Sample ITL

Sample e2v

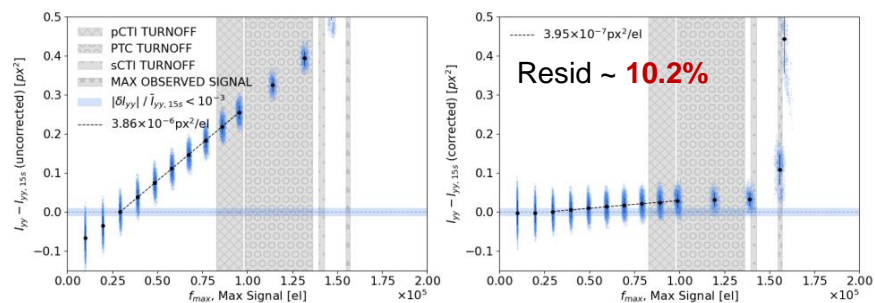
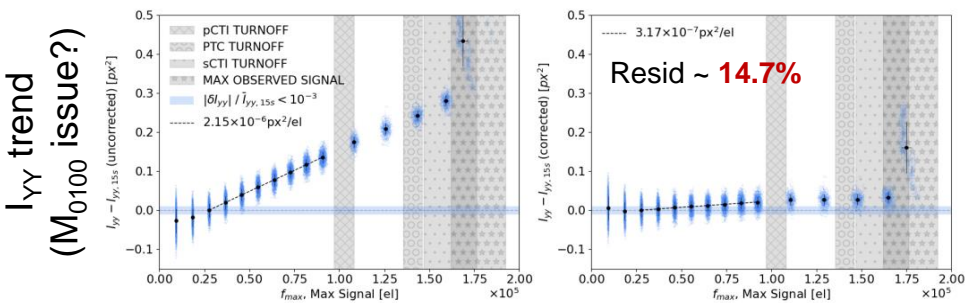
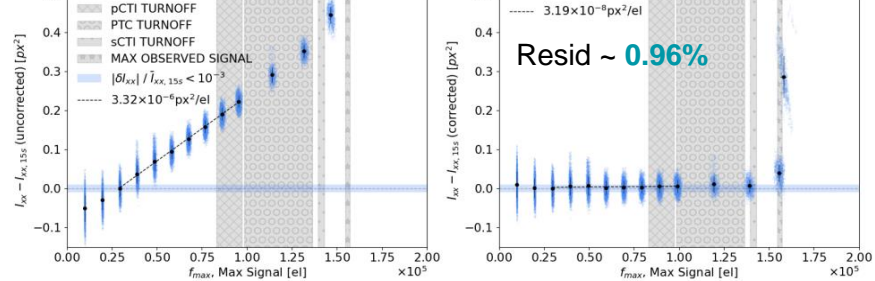
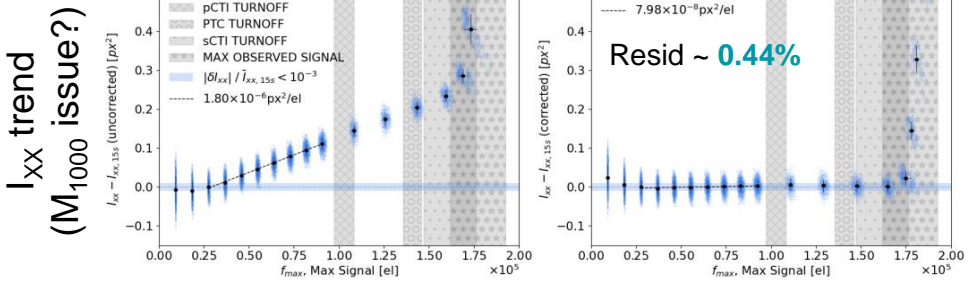
Sample e2v

Uncorrected spots

Residuals after C18 correction

Uncorrected spots

Residuals after C18 correction



Alex's careful work shows C18 (deterministic, no free parameters) algorithm systematically **under-corrects** BFE along the parallel direction. Better performance along serial direction might be coincidental. **NB:** Higher order moment problems may be present.

.. And what did other papers, exploring the limits of high fidelity correction have to say?

A selection of statements from recent publications on the state-of-the-art:

- Coulton '18: ... We can see that we meet the requirements for the Final HSC dataset, but that we need to **improve our correction by a factor of two or more** in order to reach the required levels for LSST.
- Lage '19 (arXiv:1911.09567v1): ... We also show, assuming sufficient care is paid to calculating the correction kernel, that the Coulton algorithm does in fact correct 90% or more of the BF effect on measured spots images. ... Correcting 90% of the effect should get us down near $m = 0.006$ To achieve the desired levels of $m \approx 0.001 - 0.003$, **we need to do a factor of 2-5 times better**. ... Algorithm improvement will continue as more data becomes available from a larger sample of sensors.
- Broughton et al. '23: (arXiv:2312.03115v1) Our findings also motivate a detailed study on more realistic PSF stars and how measurement errors from BF could ultimately impact cosmology and other science goals. Ultimately, it is important to characterize the sensitivity of cosmological parameters to observables biased with BFEs. Even with state-of-the-art correction techniques, **the residual effects could represent a significant component** of the systematics error budget for cosmological analyses of LSST observations.

Let's take the overlap formalism with drift calculation as *ground truth* and see how Coulton (2018) performs

- Recall Δa_{ij} are **observable** via correlations, $M_{ijj'j'}$ **are not**.
- How does the C18 algorithm reproduce $M_{ijj'j'}$?? **Test** by integrating Δa_{ij} twice to obtain the kernel K according to: $(\nabla^2 K + \Delta a)_{ij} = 0$ via successive over relaxation (SOR). Compare $(\vec{\nabla} K)_{ij}$ with corresponding elements of $M_{ijj'j'}$.
- Use BFE source levels corresponding to the flat field statistical fluctuations ($\Delta a_{00} \sim 5e-4 \text{ pix}^2$) instead of source levels near full well. Those have not been observed.
- On the following slides, the following are compared:
 - Measured Δa_{ij} are compared to Δa_{ij} based on the computed kernel $(-\nabla^2 K)$.
 - Measured overlaps $M_{ijj'j'}$ are compared to corresponding element of the kernel-based boundary displacement $\vec{\nabla} K$.

Let's take the overlap formalism with drift calculation as *ground truth* and see how Coulton (2018) performs (3)

Pixel area distortions are in **orange boxes**; overlaps ($M_{ijj'}$) are in between. **240 e⁻ source at 00..**

Top: kernel derived value
Center: Truth
Bottom: rel. dev.

C18 approach **undershoots**

M_{0100} & **overshoots**

M_{1000}

+5.25619e-06	(+3.683e-06)	+6.52923e-06	(+7.093e-06)	+5.18042e-06	(+9.942e-06)	-5.16844e-06	(+7.093e-06)	-6.51755e-06	(+3.682e-06)	-5.24511e-06
+5.95846e-06	(+3.664e-06)	+7.76161e-06	(+7.074e-06)	+4.82141e-06	(+9.923e-06)	-4.82141e-06	(+7.074e-06)	-7.76161e-06	(+3.664e-06)	-5.95846e-06
-11.7862%	(0.518%)	-15.8779%	(0.269%)	+7.44621%	(0.19%)	+7.19772%	(0.263%)	-16.0284%	(0.497%)	-11.9722%
	-8.11478e-06		-1.77815e-05		-3.31536e-05		-1.77817e-05		-8.11523e-06	
-----	-7.87257e-06	-----	-2.00414e-05	-----	-3.19322e-05	-----	-2.00414e-05	-----	-7.87257e-06	-----
	+3.07659%		-11.2761%		+3.82507%		-11.275%		+3.08233%	
+9.63867e-06	(+6.676e-06)	+1.6196e-05	(+1.918e-05)	+2.05525e-05	(+6.44e-05)	-2.05403e-05	(+1.918e-05)	-1.61841e-05	(+6.675e-06)	-9.62738e-06
+9.90367e-06	(+6.657e-06)	+1.95116e-05	(+1.916e-05)	+2.83948e-05	(+6.438e-05)	-2.83948e-05	(+1.916e-05)	-1.95116e-05	(+6.657e-06)	-9.90367e-06
-2.67576%	(0.292%)	-16.9932%	(0.102%)	-27.6187%	(0.03%)	-27.6617%	(0.0994%)	-17.0542%	(0.28%)	-2.78979%
	-8.23343e-06		-3.26028e-05		-0.00013865		-3.26029e-05		-8.2337e-06	
-----	-4.92092e-06	-----	-3.03108e-05	-----	-0.000153107	-----	-3.03108e-05	-----	-4.92092e-06	-----
	+67.3149%		+7.56163%		-9.44221%		+7.56208%		+67.3203%	
+1.53765e-05	(+8.71e-06)	+4.05653e-05	(+2.082e-05)	+0.0001266	(-0.0005305)	-0.000126587	(+2.082e-05)	-4.05533e-05	(+8.709e-06)	-1.5365e-05
+1.21903e-05	(+8.69e-06)	+3.07222e-05	(+2.08e-05)	+0.000112141	(-0.0005305)	-0.000112141	(+2.08e-05)	-3.07222e-05	(+8.69e-06)	-1.21903e-05
+26.1367%	(0.227%)	+32.0391%	(0.0949%)	+12.8934%	(-0.0037%)	+12.8824%	(0.0929%)	+32%	(0.217%)	+26.043%
	+8.24586e-06		+3.26153e-05		+0.000138662		+3.26152e-05		+8.24578e-06	
-----	+4.92092e-06	-----	+3.03108e-05	-----	+0.000153107	-----	+3.03108e-05	-----	+4.92092e-06	-----
	+67.5673%		+7.60281%		-9.43408%		+7.60269%		+67.5658%	
+9.63851e-06	(+6.676e-06)	+1.61959e-05	(+1.918e-05)	+2.05526e-05	(+6.44e-05)	-2.05402e-05	(+1.918e-05)	-1.61838e-05	(+6.676e-06)	-9.62706e-06
+9.90367e-06	(+6.657e-06)	+1.95116e-05	(+1.916e-05)	+2.83948e-05	(+6.438e-05)	-2.83948e-05	(+1.916e-05)	-1.95116e-05	(+6.657e-06)	-9.90367e-06
-2.6774%	(0.298%)	-16.9935%	(0.104%)	-27.6186%	(0.0307%)	-27.6622%	(0.102%)	-17.0553%	(0.286%)	-2.79304%
	+8.12688e-06		+1.77937e-05		+3.31658e-05		+1.77937e-05		+8.127e-06	
-----	+7.87257e-06	-----	+2.00414e-05	-----	+3.19322e-05	-----	+2.00414e-05	-----	+7.87257e-06	-----
	+3.23037%		-11.2154%		+3.86306%		-11.2151%		+3.23191%	
+5.25587e-06	(+3.684e-06)	+6.52911e-06	(+7.094e-06)	+5.1805e-06	(+9.943e-06)	-5.16818e-06	(+7.094e-06)	-6.5171e-06	(+3.683e-06)	-5.24447e-06
+5.95846e-06	(+3.664e-06)	+7.76161e-06	(+7.074e-06)	+4.82141e-06	(+9.923e-06)	-4.82141e-06	(+7.074e-06)	-7.76161e-06	(+3.664e-06)	-5.95846e-06
-11.7916%	(0.54%)	-15.8795%	(0.28%)	+7.44774%	(0.199%)	+7.19219%	(0.275%)	-16.0342%	(0.518%)	-11.9828%

Parallel Direction ↑

Serial Direction →

Let's take the overlap formalism with drift calculation as *ground truth* and see how Coulton (2018) performs (4)

Similar trend, more pronounced for a ~36ke⁻ BFE source (x148 of source on previous slide)

Top: kernel derived value
Center: Truth
Bottom: rel. dev.

C18 approach **undershoots**

M_{0100} & **overshoots**

M_{1000}

+0.000781126	(+0.0005439)	+0.00096683	(+0.00105)	+0.000764439	(+0.001474)	-0.00076443	(+0.00105)	-0.000966821	(+0.0005439)	-0.000781117
+0.00088372	(+0.0005439)	+0.00114993	(+0.00105)	+0.000712401	(+0.001474)	-0.000712401	(+0.00105)	-0.00114993	(+0.0005439)	-0.00088372
-11.6093%	0.00352%	-15.923%	0.00183%	+7.30467%	0.0013%	+7.30332%	0.0018%	-15.9239%	0.00341%	-11.6103%
	-0.00120901		-0.00264127		-0.00491096		-0.00264127		-0.00120901	
-----	-0.00116625	-----	-0.00296981	-----	-0.00473438	-----	-0.00296981	-----	-0.00116625	-----
	+3.66639%		-11.0628%		+3.72973%		-11.0628%		+3.66641%	
+0.00143227	(+0.0009883)	+0.00239908	(+0.002866)	+0.00303413	(+0.009695)	-0.00303412	(+0.002866)	-0.00239907	(+0.0009883)	-0.00143226
+0.00146917	(+0.0009883)	+0.00289147	(+0.002866)	+0.00414981	(+0.009695)	-0.00414981	(+0.002866)	-0.00289147	(+0.0009883)	-0.00146917
-2.5121%	0.00197%	-17.0291%	0.000683%	-26.8851%	0.000201%	-26.8853%	0.000673%	-17.0294%	0.00191%	-2.51272%
	-0.00123049		-0.00487196		-0.0206746		-0.00487196		-0.00123049	
-----	-0.000726704	-----	-0.00440622	-----	-0.0227421	-----	-0.00440622	-----	-0.000726704	-----
	+69.3249%		+10.5702%		-9.09085%		+10.5702%		+69.3249%	
+0.00228905	(+0.00129)	+0.00604055	(+0.003052)	+0.0188368	(-0.07902)	-0.0188368	(+0.003052)	-0.00604055	(+0.00129)	-0.00228908
+0.00180866	(+0.00129)	+0.00455379	(+0.003052)	+0.0164312	(-0.07902)	-0.0164312	(+0.003052)	-0.00455379	(+0.00129)	-0.00180866
+26.5631%	0.00153%	+32.649%	0.000649%	+14.6401%	-2.5e-05%	+14.64%	0.000639%	+32.6487%	0.00148%	+26.5626%
	+0.0012305		+0.00487197		+0.0206746		+0.00487197		+0.0012305	
-----	+0.000726704	-----	+0.00440622	-----	+0.0227421	-----	+0.00440622	-----	+0.000726704	-----
	+69.3262%		+10.5704%		-9.09081%		+10.5704%		+69.3262%	
+0.00143227	(+0.0009883)	+0.00239908	(+0.002866)	+0.00303413	(+0.009695)	-0.00303412	(+0.002866)	-0.00239907	(+0.0009883)	-0.00143226
+0.00146917	(+0.0009883)	+0.00289147	(+0.002866)	+0.00414981	(+0.009695)	-0.00414981	(+0.002866)	-0.00289147	(+0.0009883)	-0.00146917
-2.51211%	0.002%	-17.0291%	0.000694%	-26.8851%	0.000204%	-26.8853%	0.000683%	-17.0294%	0.00194%	-2.51274%
	+0.00120902		+0.00264128		+0.00491097		+0.00264128		+0.00120902	
-----	+0.00116625	-----	+0.00296981	-----	+0.00473438	-----	+0.00296981	-----	+0.00116625	-----
	+3.66721%		-11.0625%		+3.72993%		-11.0625%		+3.66722%	
+0.000781126	(+0.0005439)	+0.00096683	(+0.00105)	+0.000764439	(+0.001474)	-0.000764429	(+0.00105)	-0.00096682	(+0.0005439)	-0.000781117
+0.00088372	(+0.0005439)	+0.00114993	(+0.00105)	+0.000712401	(+0.001474)	-0.000712401	(+0.00105)	-0.00114993	(+0.0005439)	-0.00088372
-11.6093%	0.00363%	-15.923%	0.00189%	+7.30467%	0.00134%	+7.3033%	0.00186%	-15.9239%	0.00352%	-11.6104%

Parallel Direction ↑

Serial Direction →

Let's take the overlap formalism with drift calculation as *ground truth* and see how Coulton (2018) performs (5)

But cleans up substantially when we artificially dial in **x100 weaker barriers**

Top: kernel derived value
Center: Truth
Bottom: rel. dev.

C18 approach
better for
 M_{0100} &
better for
 M_{1000}

!!

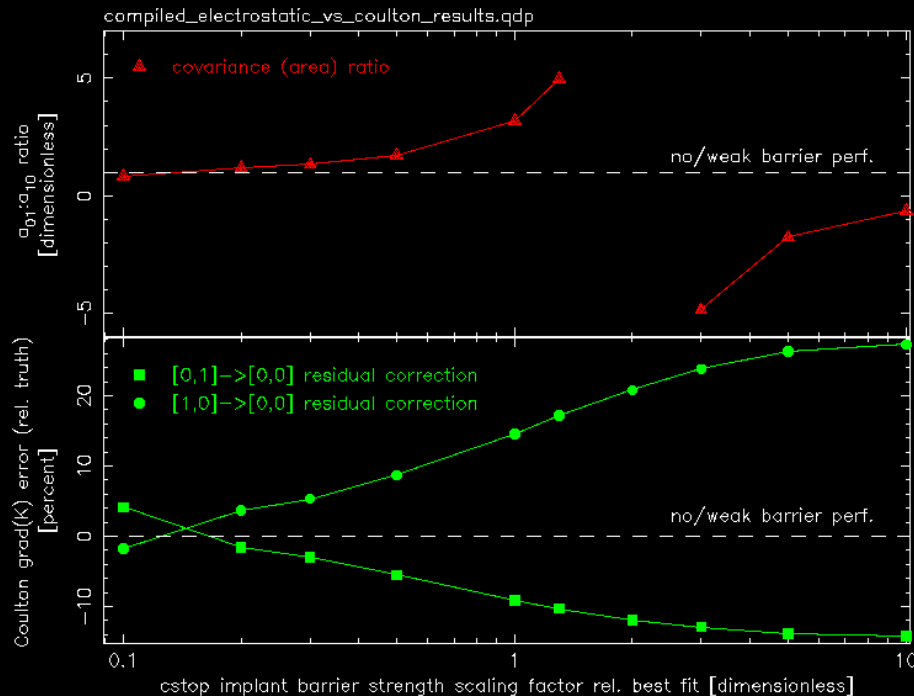
+0.000817684 +0.00091165 -10.3072%	(+0.0006038) (+0.0006037) (0.00317%)	+0.00111616 +0.00121169 -7.88365%	(+0.001219) (+0.001219) (0.00158%)	+0.00123375 +0.000774316 +59.3345%	(+0.00171) (+0.00171) (0.00112%)	-0.00123374 -0.000774316 +59.3333%	(+0.001219) (+0.001219) (0.00155%)	-0.00111615 -0.00121169 -7.88442%	(+0.0006038) (+0.0006037) (0.00307%)	+0.000817675 +0.00091165 -10.3082%
	-0.00112573 -0.0012124 -7.14891%		-0.00252477 -0.00318278 -20.674%		-0.00647404 -0.00515813 +25.5114%		-0.00252477 -0.00318278 -20.674%		-0.00112573 -0.0012124 -7.14889%	
+0.00142544 +0.00153255 -6.98943%	(+0.001216) (+0.001216) (0.0016%)	+0.00251521 +0.00317939 -20.8901%	(+0.005397) (+0.005397) (0.000363%)	+0.00518302 +0.00572452 -9.45937%	(+0.01716) (+0.01716) (0.000114%)	-0.00518301 -0.00572452 -9.45954%	(+0.005397) (+0.005397) (0.000357%)	-0.0025152 -0.00317939 -20.8904%	(+0.001216) (+0.001216) (0.00156%)	-0.00142543 -0.00153255 -6.99003%
	-0.00125186 -0.00077494 +61.5435%		-0.00525406 -0.00573459 -8.37964%		(-0.034003) (-0.033785) (+0.645278%)		-0.00525406 -0.00573459 -8.37964%		-0.00125186 -0.00077494 +61.5435%	
+0.00231136 +0.00189708 +21.8378%	(+0.001702) (+0.001702) (0.00116%)	+0.0065174 +0.0051506 +26.5366%	(+0.01691) (+0.01691) (0.000117%)	+0.033932 +0.0335411 +1.16526%	(-0.1359) (-0.1359) (-1.45e-05%)	-0.033932 -0.0335411 +1.16523%	(+0.01691) (+0.01691) (0.000115%)	-0.00651739 -0.0051506 +26.5364%	(+0.001702) (+0.001702) (0.00112%)	-0.00231135 -0.00189708 +21.8373%
	+0.00125187 +0.00077494 +61.5447%		+0.00525407 +0.00573459 -8.37947%		+0.034003 +0.033785 +0.645307%		+0.00525407 +0.00573459 -8.37947%		+0.00125187 +0.00077494 +61.5447%	
+0.00142544 +0.00153255 -6.98944%	(+0.001216) (+0.001216) (0.00163%)	+0.00251521 +0.00317939 -20.8901%	(+0.005397) (+0.005397) (0.000368%)	+0.00518302 +0.00572452 -9.45937%	(+0.01716) (+0.01716) (0.000115%)	-0.00518301 -0.00572452 -9.45954%	(+0.005397) (+0.005397) (0.000363%)	-0.0025152 -0.00317939 -20.8904%	(+0.001216) (+0.001216) (0.00158%)	-0.00142543 -0.00153255 -6.99004%
	+0.00112574 +0.0012124 -7.14812%		+0.00252478 +0.00318278 -20.6737%		+0.00647405 +0.00515813 +25.5116%		+0.00252478 +0.00318278 -20.6737%		+0.00112574 +0.0012124 -7.14811%	
+0.000817684 +0.00091165 -10.3072%	(+0.0006038) (+0.0006037) (0.00327%)	+0.00111616 +0.00121169 -7.88366%	(+0.001219) (+0.001219) (0.00163%)	+0.00123375 +0.000774316 +59.3345%	(+0.00171) (+0.00171) (0.00115%)	-0.00123374 -0.000774316 +59.3333%	(+0.001219) (+0.001219) (0.0016%)	-0.00111615 -0.00121169 -7.88445%	(+0.0006038) (+0.0006037) (0.00317%)	+0.000817675 +0.00091165 -10.3082%

Parallel Direction ↑

Serial Direction →

Fool around further by altering one of the model parameters (channel stop barrier)

- Persistent underestimation of M_{0100} and overcorrection of M_{1000} using C18 method.
- Noted improvement in C18 method when electrostatic barrier strengths are dialed down to 1% level.
- Tried scaling one of the parameters to investigate effect on the C18 errors in recovering M_{0100} etc. and tabulated observables (e.g. $\Delta a_{01} / \Delta a_{10}$).
- Result: C18 works best when either:
 - $\Delta a_{01} / \Delta a_{10} \sim 1$;
 - barriers are very weak.
- We could have asked vendors to provide sensors with $\Delta a_{01} / \Delta a_{10} \sim 1$ as a requirement !!



Mis-match of gradient-of-derived-scalar-potential ($\vec{\nabla}K$) wrt computed boundary shifts tops the short list of mechanisms that would affect *mapping of correlation measurements into boundary shifts*:

1. Shape of pixels when barrier strengths are not equal, i.e. C01/C10 \sim 3-5 (correction error +/- 10%);
2. Attraction & shift of channel potential well toward polysilicon gates as channel fills (correction error +/- 6-7% at 36ke⁻ for $N_d \sim 5e15$ cm⁻³);
3. Presence of recorded flat field level per pixel when BFE is being characterized in flat pairs: (correction error +/- 4% at 36ke⁻);
4. ~~Extended distribution of collected conversions~~ (distributed into 3x3 grid) at channel vs. modeled (point-like) spatial distribution (correction error +/- 0.06%). cf. Lage et al. '21;

- We've used a first principles-based drift simulator tool, tuned to reproduce various observable signatures/artifacts seen in LSST sensors to compute how charge is partitioned and ultimately recorded. It permits us to evaluate how current baseline correction algorithms (C18) perform and to qualitatively understand their limits.
- C18 can't be tweaked; it features a signal-independent kernel \mathbf{K} derived directly from observables and is a scalar quantity. We've shown systematic deviations between ground truth pixel boundary shifts and C18 corrections that can partially explain residual BFE terms observed by Broughton et al.
- Time to revive old/alternate BFE correction strategies?
 - Use the sparse "pixel overlap matrix" to correct pixel-by-pixel (a la Astier et al.)
 - Compute previously proposed book-keeping terms (pixel areas, astrometric shifts, 2nd moments), either for uncorrected data or representing we C18 apparently under- or over-corrects. **One option** could be for no C18 correction in ISR (but carry these pixel terms based on recorded image esp. for high S/N stars).
 - Work out a way to incorporate properties of \mathbf{K} such that $\vec{\nabla} \times \vec{\nabla} \mathbf{K} \neq 0$ (and allow it to be signal dependent while we're at it, we see this in drift calculations).

Iteratively. Maybe one step is good enough? Similar to other work, e.g. substitute $M_{ijj'}$ for $\vec{\nabla}K$ wherever it appears in C18. Otherwise, keep in mind that the $M_{ijj'}$ overlap matrix elements have more indices because they account for all area displacements between nominal and recorded pixels. 5th index may be introduced to allow overlap coefficients to evolve with signal level:

Evaluate local flux at overlap centroids using recorded image R_{mn} :
$$S_{p,q,p+\Delta i,q+\Delta j} \equiv \frac{\sum_{mn} R_{mn} (\delta_{p,m} \delta_{q,n} + \delta_{p+\Delta i,m} \delta_{q+\Delta j,n})}{\sum_{mn} (\delta_{p,m} \delta_{q,n} + \delta_{p+\Delta i,m} \delta_{q+\Delta j,n})}$$

1st order displaced signal estimate using local flux S & recorded flux R_{mn} :

$$D_{p,q,p+\Delta i,q+\Delta j}^{(0)} \equiv S_{p,q,p+\Delta i,q+\Delta j} \cdot [M_{i,j,i',j',k} R_{mn}] \cdot \left(\frac{1}{2}\right) \cdot \mathbf{W}_{p,q,\Delta i,\Delta j,i',j',m,n,k}$$

1st order estimate for incident flux F :
$$F_{mn}^{(0)} \equiv R_{mn} + \sum_{i,j} \left(D_{m,n,i,j}^{(0)} - D_{i,j,m,n}^{(0)} \right)$$

Refine displaced signal map estimate D evaluated for timeslices:

$$\begin{aligned} D_{p,q,p+\Delta i,q+\Delta j}^{(0)} &\equiv \sum_{\tau=0}^{T-1} D_{p,q,p+\Delta i,q+\Delta j,\tau}^{(0)} \\ &\equiv S_{p,q,p+\Delta i,q+\Delta j} \cdot \sum_{\tau=0}^{T-1} [M_{i,j,i',j',k} R_{mn}] \cdot \left(\frac{\tau + \frac{1}{2}}{T}\right) \cdot \mathbf{\Omega}_{p,q,\Delta i,\Delta j,i',j',m,n,k,\tau,T} \end{aligned}$$

Iterate incident flux F estimate and while displaced signal D by resolving in time slices. End with convergence condition:

$$\left[\left(\frac{\tau+1}{T}\right) \cdot R_{m,n} \right] \rightarrow \left[\left(\frac{\tau+1}{T}\right) \cdot F_{mn}^{(iter)} - \sum_{\theta=0}^{\tau-1} \left(D_{m,n,i,j,\theta}^{(iter)} - D_{i,j,m,n,\theta}^{(iter)} \right) \right]$$

$$\begin{aligned} F_{mn}^{(iter+1)} &\equiv R_{mn} + \sum_{i,j} \left(D_{m,n,i,j}^{(iter+1)} - D_{i,j,m,n}^{(iter+1)} \right) \\ D_{p,q,p+\Delta i,q+\Delta j,\tau}^{(iter+1)} &\equiv S_{p,q,p+\Delta i,q+\Delta j} \cdot \mathbf{M}_{i,j,i',j',k} \cdot \left[F_{mn}^{(iter)} \left(\frac{\tau + \frac{1}{2}}{T}\right) - \sum_{\theta=0}^{\tau-1} \left(D_{m,n,i,j,\theta}^{(iter)} - D_{i,j,m,n,\theta}^{(iter)} \right) \right] \\ &\quad \cdot \mathbf{\Omega}_{p,q,\Delta i,\Delta j,i',j',m,n,k,\tau,T} \end{aligned}$$

How can the overlap matrix $M_{ijj'}$ elements be used in a ISR process? (2)

In the previous expressions, these matrices are meant to simplify computation in nested loops over the signal- and time-resolved slices of correction. Basically, they are an amalgamation of Kronecker and Heaviside functions:

$$W_{p,q,\Delta i,\Delta j,i,j,i',j',m,n,k} \equiv \delta_{m+i,p}\delta_{n+j,q}\delta_{m+i',p+\Delta i}\delta_{n+j',q+\Delta j} \cdot \Theta(U_k - R_{mn}) \cdot \Theta(R_{mn} - L_k)$$

$$\Omega_{p,q,\Delta i,\Delta j,i,j,i',j',m,n,k,\tau,T} \equiv \delta_{m+i,p}\delta_{n+j,q}\delta_{m+i',p+\Delta i}\delta_{n+j',q+\Delta j} \cdot \Theta\left(U_k - \left(\frac{\tau+1}{T}\right)R_{mn}\right) \cdot \Theta\left(\left(\frac{\tau+1}{T}\right)R_{mn} - L_k\right).$$

Pixel distortion bookkeeping as an alternate BFE correction strategy appropriate for moments (R18)

